IJMCM
International Journal of Molecular and Cellular Medicine
p-ISSN: 2251-9637 o-ISSN: 2251-9645
Babol University of Medical Sciences
Cellular and Molecular Biology Research Center

Elucidating the Role of LINC01980 in Laryngeal Cancer: From Expression Profiling to Regulatory Network Prediction

Masoumeh Razipour[1#], Zeinab Jamali[1], Elham Ghadami[1], Saeed Sohrabpour[2], Leyla Sahebi[3], Abbas Shakoori[1,4*]

1. Department of Medical Genetics, School of Medicine, Tehran University of Medical Sciences, Tehran, Iran.
2. Otorhinolaryngology Research Center, AmirAlam Hospital, Tehran University of Medical Sciences, Tehran, Iran.
3. Family Health Research Institute, Maternal-Fetal and Neonatal Research Center, Tehran University of Medical Sciences, Tehran, Iran.
4. Department of Medical Genetics, Cancer Institute of Iran, Imam Khomeini Hospital Complex, Tehran University of Medical Sciences, Tehran, Iran.

Article type:
Original Article

Received:
2024.10.23
Revised:
2024.12.04
Accepted:
2024.12.04

ABSTRACT

Laryngeal squamous cell carcinoma (LSCC) remains a significant global health challenge despite advances in treatment. This study investigated the involvement of LINC01980, a long non-coding RNA, in LSCC pathogenesis. We conducted an integrative analysis of transcriptomic data sourced from The Cancer Genome Atlas (TCGA) and the Gene Expression Omnibus (GEO) databases to identify genes that are differentially expressed in LSCC. LINC01980 expression was evaluated in 32 matched pairs of advanced-stage LSCC and adjacent normal tissues using quantitative real-time PCR (qRT-PCR). The potential competing endogenous RNA (ceRNA) network involving LINC01980 was explored through bioinformatics analyses. Findings revealed significant upregulation of LINC01980 in LSCC tissues compared to normal adjacent tissues ($p < 0.0001$), with elevated expression in 78.125% of tumor samples. Receiver Operating Characteristic (ROC) curve analysis demonstrated LINC01980's potential as a diagnostic biomarker (AUC = 0.7666, $p = 0.0002$). While no significant correlations were found between LINC01980 expression and clinicopathological features, bioinformatics analyses identified potential LINC01980/ miRNA/ mRNA regulatory network involving hsa-let-7e-5p and hub gene MMP9. This study provides insights into LINC01980's role in LSCC and suggests its potential as a diagnostic biomarker and therapeutic target. Further research is warranted to elucidate the precise molecular mechanisms of LINC01980 in LSCC progression.

Keywords: Laryngeal Squamous Cell Carcinoma; Long Non-Coding RNA; competing endogenous RNA; LINC01980; biomarker

Cite this article: Razipour M, Jamali Z *et al*. Elucidating the Role of LINC01980 in Laryngeal Cancer: From Expression Profiling to Regulatory Network Prediction. *International Journal of Molecular and Cellular Medicine. 2025; 14(1): 517-532*.

DOI: 10.22088/IJMCM.BUMS.14.1.517

# The first two authors contributed equally to this work.

*Corresponding: Abbas Shakoori
Address: Department of Medical Genetics, School of Medicine, Tehran University of Medical Sciences, Tehran, Iran
E-mail: shakooria@sina.tums.ac.ir

[DOI: 10.22088/IJMCM.BUMS.14.1.517]

Introduction

Laryngeal squamous cell carcinoma (LSCC), accounting for approximately 95% of laryngeal malignancies, is the second most prevalent form of head and neck squamous cell carcinoma (HNSCC). Despite advancements in treatment modalities, patient outcomes remain suboptimal, with 188,960 new cases and 103,216 deaths reported worldwide in 2022 (1, 2). These statistics underscore the urgent need for improved approaches to LSCC management, particularly through the elucidation of the underlying molecular mechanisms driving its development and progression.

Long non-coding RNAs (lncRNAs) have emerged as key regulators of cellular homeostasis and significant contributors to tumor biology across various human cancers (3, 4). These non-protein coding transcripts, exceeding 200 nucleotides in length, influence numerous biological functions such as cell growth, programmed cell death, epithelial-to-mesenchymal transition (EMT), invasion, migration, angiogenesis, and differentiation (5). While numerous studies have investigated lncRNAs function in laryngeal cancer, the expression patterns and functional roles of many lncRNAs in LSCC pathogenesis remain poorly understood.

We employed a systematic, multi-step approach to identify promising lncRNA candidates in LSCC through computational analyses of The Cancer Genome Atlas (TCGA) and Gene Expression Omnibus (GEO) databases. Given that upregulated lncRNAs present several advantages, such as being more readily detectable as diagnostic biomarkers and serving as potential therapeutic targets for inhibition, our focus was directed towards these upregulated lncRNAs. By applying stringent criteria (Log2FC≥3), we identified eight significantly upregulated lncRNAs. Among these candidates, LINC01980 was selected for further investigation based on three critical factors: its notable upregulation in our bioinformatics analysis, its documented oncogenic roles in other cancer types, and the lack of prior research concerning its role in head and neck cancer.

Long intergenic non-protein coding RNA 1980 (LINC01980) has demonstrated emerging significance in tumor biology, particularly in esophageal squamous cell carcinoma (ESCC) (6, 7) and hepatocellular carcinoma (HCC) (8, 9). In ESCC, LINC01980 upregulation correlates with deeper cancer invasion, lymph node metastasis, advanced TNM stage, and poor prognosis. In vitro and in vivo experiments demonstrate that LINC01980 promotes ESCC growth, proliferation, and survival while inhibiting apoptosis through two distinct mechanisms: upregulation of GADD45A expression and sponging of miR-190a-5p to regulate MYO5A expression (6, 7). In HCC, the canonical TGF-β/SMAD signaling pathway induces the expression of LINC01980, which promotes metastasis through the miR-376b-5p/E2F5 axis (8). Additionally, LINC01980 has been identified as a risk factor in pancreatic adenocarcinoma (PAAD) and stomach adenocarcinoma (STAD) (10).

Given LINC01980's unexplored role in LSCC, our study aimed to investigate its expression using quantitative real-time polymerase chain reaction (qRT-PCR) and analyze its correlation with clinicopathological features of LSCC patients. We utilized bioinformatics databases and systems biology approaches to explore potential mechanisms of LINC01980 in LSCC, focusing on its function as a competing endogenous RNA (ceRNA). This research seeks to elucidate LINC01980's role in LSCC pathogenesis, potentially revealing novel biomarkers for early diagnosis, targeted therapies, and accurate prognosis, ultimately contributing to enhanced treatment efficacy and improved patient survival rates.

[DOI: 10.22088/IJMCM.BUMS.14.1.517]

Materials and methods

Patients and tissue samples

This study examined 32 matched pairs of LSCC and adjacent normal tissue samples, all from patients with stage III or IV disease. Specimens were obtained from the Otorhinolaryngology Research Center's tumor bank at AmirAlam Hospital, Tehran, Iran. The research protocol received institutional ethics committee approval (Approval code: IR.TUMS.AMIRALAM.REC.1401.034), and participants provided documented consent for research use of their biological specimens.

Exclusion criteria included prior chemotherapy, radiotherapy, or immunotherapy, as well as any history of previous or secondary malignancies. Expert pathologists assessed all samples to confirm disease staging based on established clinicopathological criteria. This rigorous selection process ensured a well-defined patient cohort for investigating LSCC at advanced stages.

Transcriptome expression profiling in LSCC through GEO and TCGA data analysis

Data source and analysis

The transcriptomic data from the TCGA-LSCC project (extracted from 'TCGA HNSC' project) was obtained from the Genomic Data Commons (GDC) portal (https://portal. gdc.cancer. gov/analysis_ page?app=Projects) utilizing the GDCRNATools package within R 4.3.2 software. This dataset comprised gene expression profiles from 116 LSCC & 12 normal samples. Additionally, we analyzed the GSE130605 dataset from the GEO database (https://www.ncbi.nlm.nih.gov/geo/), which was based on the GPL20301 platform, Public on June 09, 2015. This dataset comprised whole transcriptome sequencing data from 50 matched pairs of LSCC and adjacent normal tissues. We processed this data using the GEO2R tool.

This dual-database approach allowed for a robust and comprehensive analysis of transcriptomic changes in LSCC, providing insights from both large-scale (TCGA) and focused (GEO) datasets.

Identification of DEmRNAs and DElncRNAs

The analysis of the TCGA-LSCC dataset was conducted to identify differentially expressed genes, including both mRNAs and lncRNAs in tumor samples compared to normal laryngeal tissue samples. This analysis was performed using R software with the TCGAbiolinks package. Genes exhibiting a log2 fold change (log2FC) of ≥ 2 (for mRNAs) and 3 (for lncRNAs) (11) and an adjusted *p*-value of less than 0.05 were selected for further investigation. Additionally, the GSE130605 dataset was examined to uncover differentially expressed genes (mRNAs and lncRNAs) between LSCC and paired normal adjacent tissues. This analysis utilized GEO2R, which employs the DESeq2 algorithm. The criteria for selecting differentially expressed genes included a significance level cut-off of less than 0.05 and a log2 fold change threshold of ≥2 (for mRNAs) and 3 (for lncRNAs) (11). To minimize the occurrence of false positive results, the analysis outcomes from the GSE130605 dataset and the TCGA-LSCC project were combined, and intersection values were derived utilizing the Venn diagram tool (http://bioinformatics.psb.ugent.be/webtools/Venn/). This process led to the identification of the final differentially expressed mRNAs (DEmRNAs) and lncRNAs (DElncRNAs).

Construction of ceRNA regulatory network hypothesis

A total of eight upregulated DElncRNAs were identified from earlier analyses. Among these, LINC0 1980 was chosen as a key component for constructing the lncRNA/miRNA/mRNA regulatory network.

[DOI: 10.22088/IJMCM.BUMS.14.1.517]

Expression study

Fresh frozen tissue samples (50 mg) were processed for total RNA extraction using Kiazol Reagent (KIAZIST Life Sciences, Iran) according to the manufacturer's guidelines. RNA quantity and purity were assessed using a Nanodrop 2000C spectrophotometer (Thermo Scientific, USA), while RNA integrity was confirmed by visualizing the 28S:18S rRNA ratio through agarose gel electrophoresis. The ExcelRT^{TM} Reverse Transcription Kit II (SMOBIO Technology, Inc., Taiwan) was employed for cDNA synthesis. Quantitative real-time PCR (qRT-PCR) was performed to measure relative lncRNA expression levels in cancerous and non-cancerous tissues using RealQ Plus 2x Master Mix Green (Amplicon, Denmark) on a Roche LightCycler® 96 System. The PCR protocol consisted of initial denaturation at 95°C for 15 minutes, followed by 45 cycles of 95°C for 20 seconds and 62°C for 50 seconds. Melt curve analysis (60-99°C) and agarose gel electrophoresis of PCR products were used to verify primer specificity and reaction efficiency. The RPL30 gene served as the reference for expression normalization, having been previously validated as a stable housekeeping gene for quantitative gene expression analyses in HNSCC. Primer sequences for LINC01980 were: Forward 5′- GGTTTGACTGACTCCTGGCAAG -3′ and Reverse 5′- GCAGGAATCCA-GGGCATGTTC -3′; for RPL30: Forward 5′-TGGCTATCATTGATCCAGGTGAC-3′ and Reverse 5′-GCAGGTTTAAGGTTTGCAGGTG-3′. Each sample was tested in duplicate, with relative expression calculated using the comparative CT method (2^-ΔΔCT).

Construction of the protein-protein interaction (PPI) network for upregulated differentially expressed mRNAs

To explore the physical and functional interactions among upregulated mRNAs (and their corresponding proteins), we utilized the STRING 12.0 database, July 26, 2023 (https://string-db.org). This resource employs various active interaction sources, including text mining, experimental data, existing databases, co-expression analyses, neighborhood information, gene fusion events, and co-occurrence metrics. For the construction of the PPI network, a minimum confidence score threshold of 0.400 was established. The visualization of the resulting PPI network was performed using Cytoscape software version 3.10.2.(release date 3/26/2024). In selecting hub genes from the PPI network for further analysis, we applied specific criteria: we identified 10 hub genes based on i) the highest degree of connectivity (ranging from 28-54) and ii) the highest corresponding Betweenness Centrality values (between 951.7 and 5308.7).

Functional and pathway enrichment analysis of hub-genes

The Enrichr tool (http://amp.pharm.mssm.edu/Enrichr/) was utilized to investigate the functional annotation and enrichment of pathways from the Kyoto Encyclopedia of Genes and Genomes (KEGG), along with conducting MSigDB Hallmark enrichment analysis for 10 hub genes that exhibited common upregulation. A significance threshold was established, with *p*-values and adjusted *p*-values set at <0.05.

Construction of the ceRNA Network

The potential interactions between LINC01980 and miRNAs were predicted using DIANA-LncBase v3, released 2020 Jan (https://diana.e-ce.uth.gr/lncbasev3/interactions). Additionally, the interactions between miRNAs and their corresponding target genes were identified using miRTarBase 2020 (https:// awi. cuhk. edu.cn/~miRTarBase/miRTarBase_2025/ php/index.php). Following this analysis, DEmRNAs that interacted with common miRNAs associated with LINC01980 were selected for further examination. To

[DOI: 10.22088/IJMCM.BUMS.14.1.517]

visualize the potential regulatory networks involving the LINC01980/miRNA/mRNA pathway, Cytoscape software (version 3.10.1) was employed.

Statistical Analysis

In this study, all statistical analyses were performed using GraphPad Prism version 9.1.0. The results are expressed as mean values with their corresponding standard deviations. To evaluate the normality of the data distribution, both the Kolmogorov-Smirnov test and the Shapiro-Wilk test were employed. The Wilcoxon test was utilized to compare the relative expression levels of lncRNA between LSCC tissues and their corresponding normal adjacent tissues. Furthermore, the relationship between lncRNA expression levels and various clinicopathological characteristics was assessed using the unpaired t-test and the non-parametric Mann-Whitney U test. To determine the diagnostic efficacy of the investigated lncRNA as a potential biomarker, a receiver operating characteristic (ROC) curve was generated. A p-value threshold of less than 0.05 was established to denote statistical significance.

Results

Differential expression analysis of mRNAs and lncRNAs

We conducted a comprehensive analysis of transcriptomic data from both the TCGA-LSCC project and the GSE130605 dataset. Comparison of gene expression profiles between tumor and normal or adjacent tissues revealed significant differences. In the GSE130605 dataset, we identified 320 upregulated DEmRNAs and 16 upregulated DElncRNAs. The TCGA-LSCC project analysis yielded 1365 upregulated DEmRNAs and 438 upregulated DElncRNAs. Upon integration of these datasets, our final results showed 219 common upregulated DEmRNAs and 8 common upregulated DElncRNAs. These findings are visually represented in Figure 1 and Table 1.

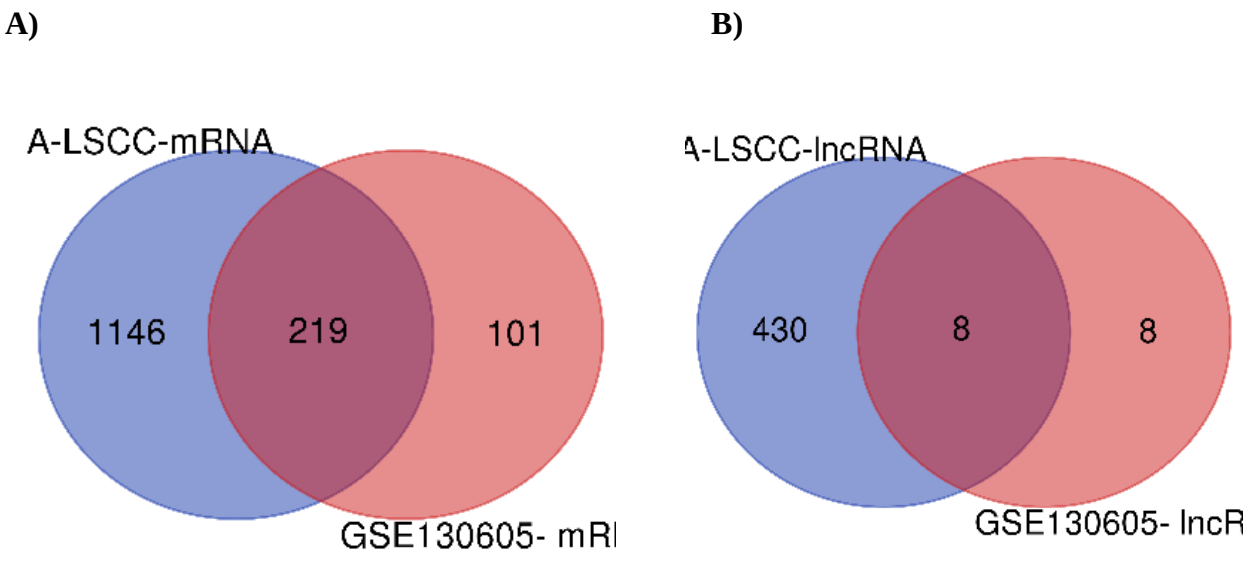

Fig. 1. Venn diagrams of intersected deferentially expressed sequencing data. a. 1466 upregulated DEmRNAs, b. 446 upregulated DElncRNAs

[DOI: 10.22088/IJMCM.BUMS.14.1.517]

Table 1. Common DE-RNAs from TCGA-LSCC and GSE130605 datasets

Common DE-RNAs	Symbols
Common DEmRNAs based on log2 FC ≥ 2	PNCK, KIF26B, SLC6A2, CCNA1, DMP1, CXCL14, PLAU, KLK14, COL22A1, CNGB1, MMP13, HOXC13, NETO2, AQP9, SLCO1B3, CALB1, LY6K, GJA1, B4GALNT1, GPNMB, ASPRV1, TCHH, ZIC2, COL1A1, UCHL1, FBN2, DNAH17, HTR7, CREG2, SYT12, BCHE, VAX2, PTHLH, P4HA3, IL24, TDRD5, DNMT3B, PNLDC1, ADAM23, RAG1, AKR1B15, KLHDC7B, NOTUM, TENM2, CDC6, CHI3L1, CACNA1B, PKHD1, CXCL11, ADAMTS2, CXCL8, FN1, KRT17, IFI27, CDSN, RPE65, CELSR3, IL1A, FST, COL5A2, UCN2, HOXA10, THY1, SPP1, GPR176, OSM, OLR1, NEFL, SPRR4, PAPPA2, PCDH15, SLCO1A2, LRRC15, MAP7D2, ERC2, NPNT, DSC1, ACP7, IL36G, LAMA1, TUBB3, SLC24A2, SLC7A11, TFRC, CHST2, ULBP1, IGFL2, NELL2, CHIT1, PCSK9, LAMA3, SLC11A1, OASL, MMP1, CBX2, COL8A1, MMP12, HMGA2, EMX1, ISG15, ADAMTS12, AMTN, MMP11, CPA6, XCL1, PLPP4, ZNF695, NXPH4, ARSI, PDPN, SDS, COL3A1, LUM, KREMEN2, SYNDIG1, ALOXE3, TMEM158, ZNF114, MMP3, IGF2BP2, SERPINH1, PNPLA3, FAP, BST2, INHBA, NTRK2, IFI6, LOXL2, POSTN, CYP27B1, POTEF, TREM2, CPXM1, LCE3D, HOXD10, RAB3B, TSPAN10, WNT2, CSMD2, GRIN2D, STEAP1B, P3H2, SCN2A, GPRIN1, CNTN1, KCNG3, PTH2R, LIPG, KRT16, FEZ1, DLX5, DPF1, PIWIL2, APLN, CNTNAP2, PLA2G7, MFAP2, HOXA9, MTCL1, CCDC87, NRIP3, ODC1, RAC3, SALL4, COL4A6, CXCL10, GDPD2, SERPINE1, COL4A1, SLC13A5, C1QTNF12, KRTDAP, ERVMER34-1, SPINK6, LAMC2, CXCL5, NRCAM, COL6A3, SYT14, FPR2, TRPV3, SHISA2, SPRR2G, IL1B, STC2, TDO2, S100A7A, SHOX2, COL5A1, COL11A1, GRK7, TREM1, HKDC1, CTHRC1, LRAT, TM4SF19, HOXB7, TFPI2, RBP1, ONECUT2, TGFBI, HAP1, COL27A1, PHLDB2, OGDHL, SH2D5, COL1A2, DUSP9, HSD17B6, ADD2, APOC1, SCN9A, COL12A1, ROS1, KRT75, ARTN, SPOCD1, MMP9, ESM1
Common DElncRNAs based on log2 FC ≥ 3	LINC01694, LINC02042, SLC12A5-AS1, LINC01322, LINC01206, LCAL1, ZFPM2-AS1, LINC01980

The LINC01980/miRNA/mRNA regulatory network hypothesis

Analysis of two transcriptomic datasets revealed eight consistently upregulated lncRNAs: LCAL1, LINC01322, SLC12A5-AS1, LINC01206, LINC01980, ZFPM2-AS1, LINC01694, and LINC02042. Among these, LINC01980 emerged as a particularly compelling candidate for further investigation due to three key factors: its notable upregulation in our bioinformatics analysis, its documented oncogenic roles in other cancer types, and the lack of prior research concerning its role in head and neck cancer. Figure 2 illustrates the graphical workflow of our research strategy for selecting LINC01980. Subsequently, we focused on characterizing the LINC01980/miRNA/mRNA regulatory network to investigate its potential role in LSCC pathogenesis.

[DOI: 10.22088/IJMCM.BUMS.14.1.517]

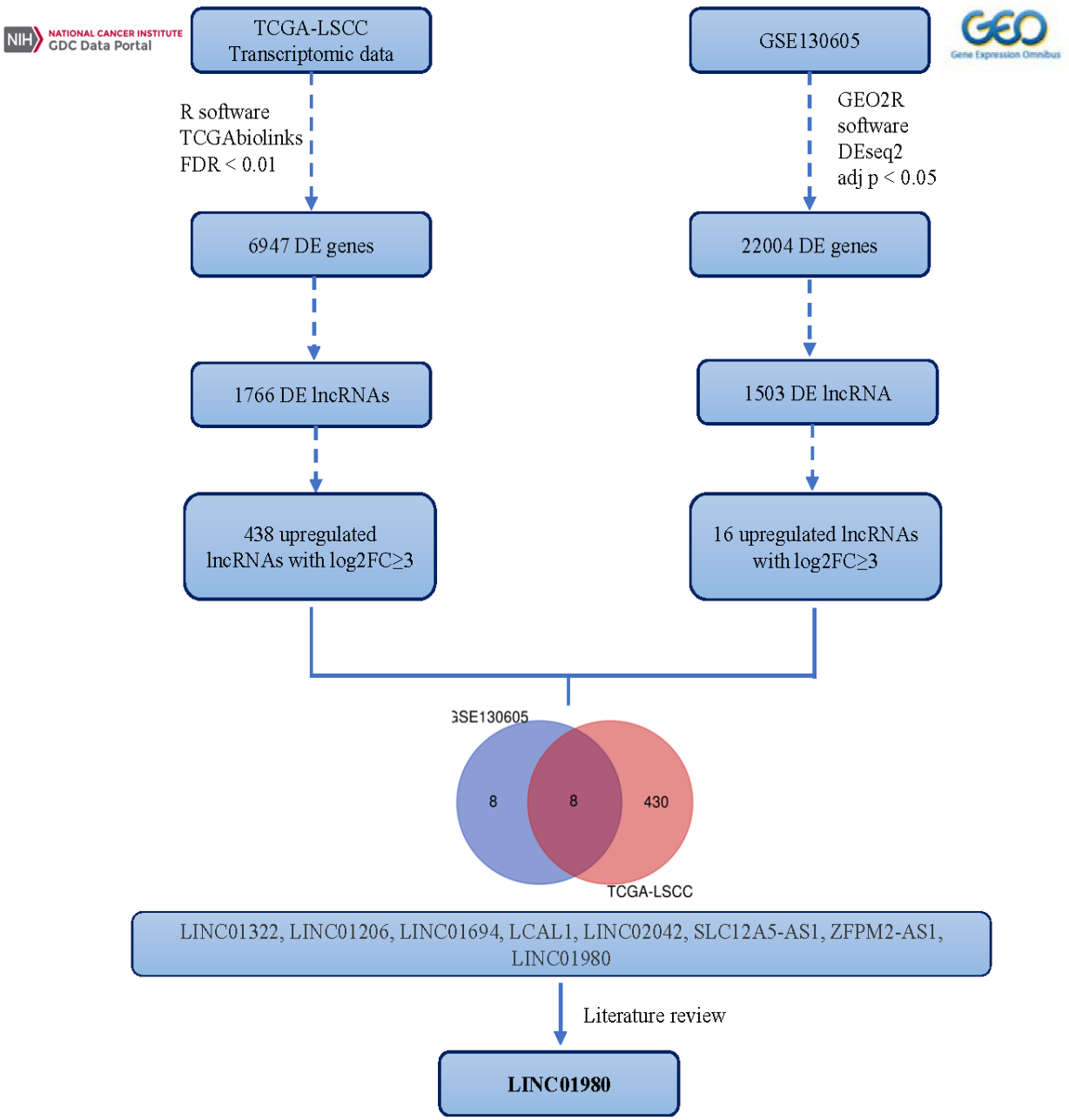

Fig. 2. The graphical workflow of the research strategy for selecting LINC01980

LINC01980 expression analysis in LSCC patients

We evaluated LINC01980 expression levels in 32 advanced-stage (III and IV) LSCC tissue samples and their corresponding non-cancerous tissues. The analysis revealed a statistically significant upregulation of LINC01980 in tumoral tissues compared to non-cancerous counterparts ($p < 0.0001$) (Fig. 3). Moreover, elevated LINC01980 expression was observed in 78.125% (25/32) of tumor samples relative to their matched normal adjacent tissue.

[DOI: 10.22088/IJMCM.BUMS.14.1.517]

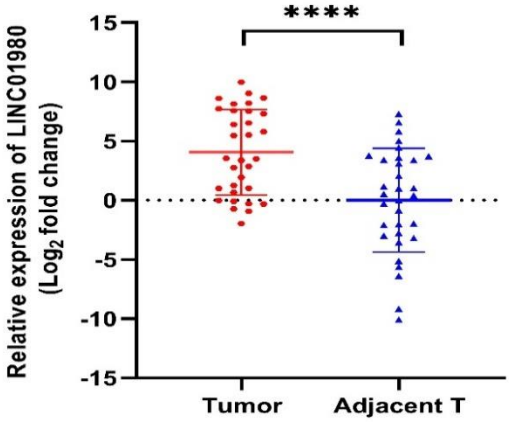

Fig. 3. LINC01980 expression in LSCC. Higher expression of LINC01980 (****p < 0.0001) in LSCC tissues compared with adjacent non-cancerous tissues

Analysis of LINC01980 expression in relation to clinicopathological features in LSCC patients

We examined the potential associations between LINC01980 expression levels and various clinicopathological characteristics of LSCC patients. The analyzed features, summarized in Table 2, included age, tumor size, disease stage, histological grade, lymph node metastasis (LNM) status, presence of lymphovascular/perineural invasion, and patient smoking/drinking history. Statistical analysis revealed no significant correlations between elevated LINC01980 expression and any of the examined clinicopathological parameters (all $p > 0.05$, Table 2).

Diagnostic potential of LINC01980 expression profile in LSCC

To assess the diagnostic and prognostic significance of LINC01980 expression levels in differentiating LSCC tissues from adjacent normal tissues, a ROC curve analysis was conducted (Fig. 4). The findings from this ROC curve analysis suggest that LINC01980 expression levels are a promising biomarker for distinguishing LSCC patients, exhibiting a sensitivity of 71.88% and a specificity of 87.5%. The area under the curve (AUC) was determined to be 0.7666, with a 95% confidence interval ranging from 0.6418 to 0.8914, and a statistically significant *p*-value of 0.0002.

PPI network for upregulated common DEmRNAs and Enrichment analysis

Following the bioinformatics and expression analysis, it was determined that LINC01980 exhibited a significant increase in expression levels within LSCC tissues compared to adjacent non-cancerous tissues. We propose that there exist critical hub genes that are upregulated and regulated by specific miRNAs, with LINC01980 functioning as a ceRNA associated with these miRNAs. Consequently, we examined the regulatory network involving LINC01980, miRNAs, and mRNAs, wherein LINC01980 is upregulated alongside both downregulated and upregulated miRNAs and mRNAs, respectively. The protein-protein interaction (PPI) network for the common upregulated mRNAs was constructed utilizing the STRING database. The resultant network comprised 167 nodes and 823edges (Fig. 5 and Table 3). Also, we identified 12 clusters/modules, with the largest module comprising 31 nodes and 278 edges. In the subsequent phase of the analysis, 10 Hub genes were pinpointed based on their degree and Betweenness Centrality scores

[DOI: 10.22088/IJMCM.BUMS.14.1.517]

utilizing Cytoscape version 3.10.2 (Table 4). The analysis of enrichment concerning the functions and pathways linked to these hub genes revealed their participation in several crucial biological pathways. These include pathways associated with cancer, the IL-17 signaling pathway, the TNF signaling pathway, interactions between extracellular matrix (ECM) and receptors, EMT, angiogenesis, and pathways related to inflammatory responses (Fig. 6 a and b).

Table 2. Relationship Between LINC01980 Expression and Clinicopathological Features in LSCC Patients.

Characteristic	Number of patients (%)	Difference between means (A - B) ± SEM	95% confidence interval	P-value
Gender Male Female	32 (100%) 0 (0%)	-	-	-
Age (years) < 57 ≥ 57	16 (50%) 16 (50%)	-1.407 ± 1.272	-4.005 to 1.191	0.2388[a]
Tumor diameter < 4 ≥ 4	15 (46.875%) 17 (53.125%)	-1.740 ± 1.261	-4.315 to 0.8355	0.1890[a]
Differentiation Well + Moderate Poor	25 (78.125%) 7 (21.875%)	1.340 ± 1.550	-1.827 to 4.506	0.3464[a]
Lymphovascular invasion Yes No	9 (28.125%) 23 (71.875%)	0.4253 ± 1.441	-2.518 to 3.368	0.7700
Perineural invasion Yes No	14 (43.75%) 18 (56.25%)	-1.304 ± 1.286	-3.931 to 1.322	0.3186
Lymph node metastasis Yes No	16 (50%) 16 (50%)	0.6344 ± 1.293	-2.005 to 3.274	0.6272
Clinical stage III IV	17 (53.125%) 15 (46.875%)	-1.019 ± 1.287	-3.647 to 1.610	0.4349
Smoking Yes No	30 (93.75%) 2 (6.25%)	4.132 ± 2.572	-1.121 to 9.386	0.1187
Alcohol consumption Yes No	3 (9.375%) 29 (90.625%)	-0.2592 ± 2.226	-4.805 to 4.286	0.9081

The P values reported in the table were derived from the unpaired t-test, except for those marked with ([a]), which were obtained using the non-parametric Mann-Whitney U test.

[DOI: 10.22088/IJMCM.BUMS.14.1.517]

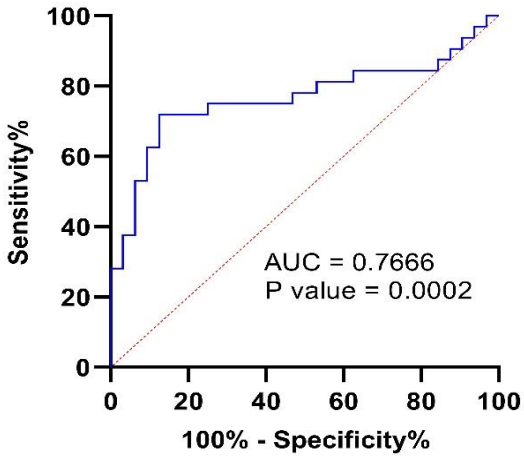

Fig. 4. The receiver operating characteristic (ROC) curve of LINC01980 expression for discrimination of LSCC from adjacent tissues. AUC indicates area under the ROC curve.

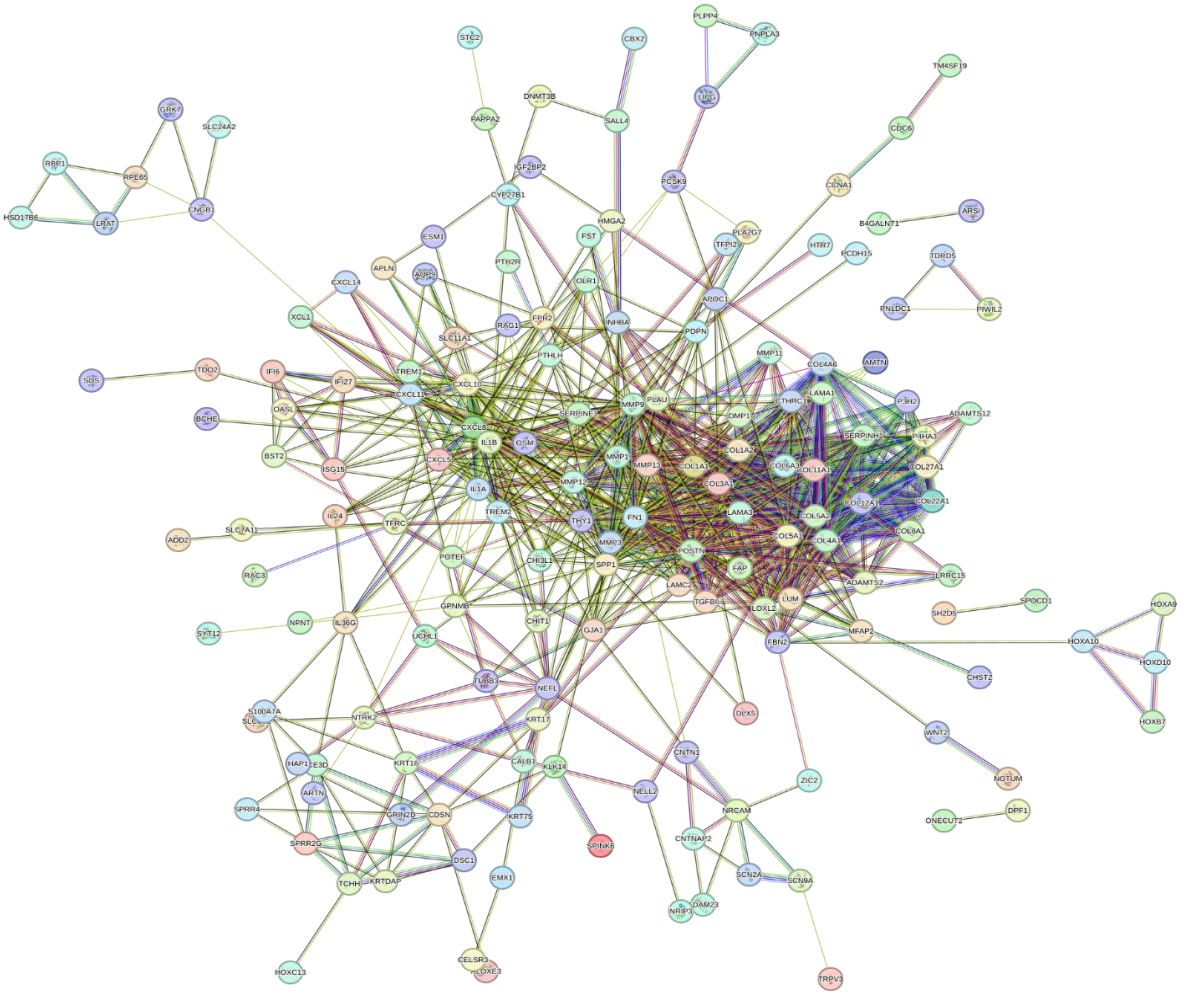

Fig. 5. The PPI network for upregulated common mRNAs.

[DOI: 10.22088/IJMCM.BUMS.14.1.517]

Table 3. Topological parameters for the network

Summary Statistics	
Number of nodes	167
Number of edges	823
Avg. number of neighbors	9.856
Network diameter	9
Network radius	1
Characteristic path length	2.417
Clustering coefficient	0.224
Network density	0.030
Connected components	5
Multi-edge node pairs	0
Number of self-loops	0
Analysis time (sec)	0.412

Table 4. 10 Hub genes in the PPI network

Top 10 in network string data ranked by Degree			Betweenness centrality score
1	IL1B	47	5308.794224
2	FN1	54	4164.85655
3	MMP9	41	1822.977712
4	SPP1	34	1709.462699
5	COL1A1	50	1397.048211
6	MMP3	31	1378.757999
7	COL3A1	41	1223.263587
8	POSTN	36	1138.902654
9	CXCL8	33	1098.805001
10	SERPINE1	28	951.7557463

Construction of the Potential ceRNA Network

Utilizing DIANA tool (https://diana.e-ce.uth.gr/lncbasev3/interactions) analysis, it was determined that 8 miRNA (hsa-let-7e-5p, hsa-miR-106b-5p, hsa-miR-1287-5p, hsa-miR-193b-5p, hsa-miR-19b-1-5p, hsa-miR-33b-3p, hsa-miR-497-3p, hsa-miR-942-5p) exhibited potential interactions with LINC01980. Additionally, an investigation using miRTarBase revealed that out of 10 hub genes derived from the common upregulated DEmRNAs, only MMP9 possess interaction sites with hsa-let-7e-5p. Consequently, LINC01980/hsa-let-7e-5p/MMP9 network could be proposed as a potential ceRNA regulatory network in the progression of LSCC.

[DOI: 10.22088/IJMCM.BUMS.14.1.517]

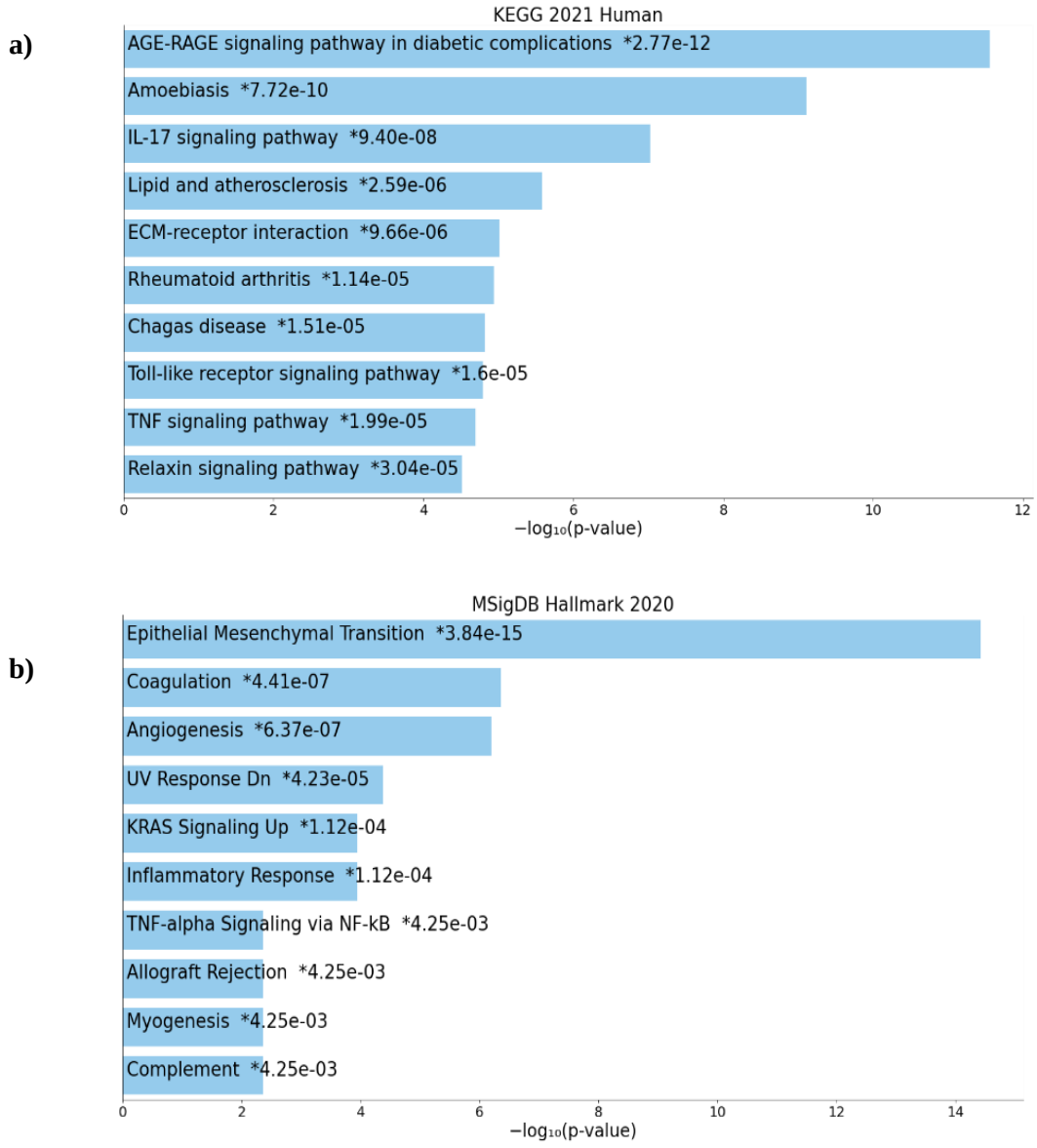

Fig. 6. a) The KEGG and **b)** MSigDB Hallmark, enrichment analyses of ten hub genes and corresponding p-values, conducted using the Enrichr database

Discussion

This study provides novel insights into the role of LINC01980 in LSCC, a significant subset of head and neck carcinoma. Our findings contribute to the growing body of evidence highlighting the importance of lncRNAs in cancer biology and their potential as diagnostic biomarkers and therapeutic targets.

Our integrated analysis of transcriptomic data from TCGA-LSCC and GSE130605 datasets, spanning LSCC samples across all stages (predominantly stages III and IV), revealed consistent upregulation of LINC01980 in LSCC tissues. This finding was validated through qRT-PCR analysis of 32 matched pairs of advanced-stage LSCC and adjacent normal tissues, demonstrating approximately 16-fold increase in

[DOI: 10.22088/IJMCM.BUMS.14.1.517]

LINC01980 expression in tumor samples ($p < 0.0001$). The observed upregulation in 78.125% of tumor samples underscores the potential importance of LINC01980 in LSCC pathogenesis. These results align with previous studies implicating LINC01980 in other cancer types, including ESCC (6, 7) and HCC (8, 9), suggesting a broader role in oncogenesis through shared molecular mechanisms. While our broader bioinformatics analysis provided a comprehensive overview of lncRNA expression patterns, the experimental phase focused specifically on stages III and IV due to patient sample availability, introducing some methodological heterogeneity that we acknowledge as a limitation of the present study.

The diagnostic potential of LINC01980 was demonstrated through ROC curve analysis, which showed promising capability in distinguishing LSCC tissues from adjacent normal tissues (AUC = 0.7666, p= 0.0002). The high specificity (87.5%) and sensitivity (71.88%) observed suggest that LINC01980 expression levels could serve as a valuable biomarker for LSCC detection. This finding is particularly significant given the current challenges in early LSCC diagnosis. However, as our study focused on advanced-stage (III and IV) cases, future research should investigate LINC01980 expression patterns across all LSCC stages to determine its efficacy as an early diagnostic marker.

Notably, our analysis revealed no significant correlations between LINC01980 expression levels and various clinicopathological features, including age, tumor size, histological grade, lymph node metastasis status, and patient history. This contrasts with findings in other cancer types where LINC01980 expression has been associated with aggressive clinicopathological features (6-9). This discrepancy may be attributed to our homogeneous patient cohort of high-stage LSCC cases, warranting further studies with a more diverse patient population. Additionally, it is worth noting that the relatively small sample size in our study may also contribute to the lack of observed correlations.

Our bioinformatic analyses suggest that LINC01980 may function as a ceRNA in LSCC. Specifically, we identified a potential regulatory pathway involving LINC01980/hsa-let-7e-5p/MMP9, which provides a framework for understanding LINC01980's influence on gene expression and its contribution to LSCC pathogenesis.

The human let-7 miRNA family comprises 13 distinct members and is recognized as a critical tumor suppressor gene family, playing pivotal roles in regulating cellular pluripotency, proliferation, and differentiation (12). The role of hsa-let-7e-5p exhibits complex and tissue-specific patterns in various cancers. In several cancer types, including breast cancer (13), non-small-cell lung cancer (NSCLC) (14) and epithelial ovarian cancer (15), downregulation of hsa-let-7e-5p correlates with increased aggressiveness and poor prognosis. Conversely, elevated hsa-let-7e-5p expression has been observed in hepatocellular carcinoma (16), colon cancer (17), and esophageal cancer (18). While hsa-let-7e-5p levels notably increased in oral tongue squamous cell carcinoma, particularly among young patients (19), recent studies have revealed its downregulation in HNSCC tissues and aggressive cells, where it suppresses cancer progression and metastasis by targeting CCR7 (20). Additionally, significant downregulation of let-7e-5p has been observed in exosomes derived from LSCC cell lines compared with parental cells (21).

Matrix metalloproteinase-9 (MMP-9), confirmed as a direct target of miRNA let-7e (22), plays a crucial role in HNSCC progression through multiple mechanisms. MMP9 facilitates tumor invasion by degrading type IV collagen, promotes angiogenesis, and influences cell migration through interactions with CD44 and

[DOI: 10.22088/IJMCM.BUMS.14.1.517]

αvβ3 (23). Its clinical significance is demonstrated by survival data showing significantly lower 5-year survival rates (61% versus 92.9%) in patients with elevated MMP9 expression (24). Moreover, MMP9 serves as a predictor of tumor recurrence and may indicate increased risk of progression from oral dysplasia to squamous cell carcinoma (23). In laryngeal cancer specifically, elevated MMP9 expression strongly correlates with advanced TNM stage and poor prognosis, highlighting its role in disease progression and metastasis (25, 26).

The critical role of MMPs in ECM degradation highlights their significance in EMT, which directly influences mechanisms underlying chemoresistance and metastasis. These characteristics have positioned MMPs as promising therapeutic targets in cancer research. However, efforts to develop MMP inhibitors have faced significant challenges. Although several MMP inhibitors, such as Batimastat, Marimastat, Tanomastat, and Prinomastat, have been formulated and assessed in clinical trials, their effectiveness has been constrained by toxicity resulting from inadequate selectivity and broad-spectrum activity (27, 28). To date, none of these inhibitors have received approval from the Food and Drug Administration (FDA) for cancer treatment. In this regard, targeting the LINC01980/hsa-let-7e-5p/MMP9 axis may offer a novel strategy for modulating MMP function in LSCC.

Our proposed ceRNA mechanism aligns with the growing understanding of lncRNAs as important gene expression regulators. By sequestering specific microRNAs, LINC01980 may indirectly modulate the expression of key genes involved in tumor progression. The LINC01980/hsa-let-7e-5p/MMP9 axis represents a potentially important pathway in LSCC pathogenesis, though further functional studies are needed to fully elucidate this mechanism. To validate the LINC01980/hsa-let-7e-5p/MMP9 axis, several experimental approaches would be necessary. These include luciferase reporter assays to confirm direct binding interactions, RNA pull-down and RNA immunoprecipitation (RIP) assays to verify interaction between RNA molecules and proteins, Western blot analysis to assess MMP9 expression following LINC01980 modulation, and rescue experiments to confirm the function of the target gene. These validations would provide crucial mechanistic evidence for our proposed regulatory pathway.

While our focus was on upregulated lncRNAs as potential diagnostic and therapeutic targets, we acknowledge that downregulated lncRNAs may also play significant roles in LSCC pathogenesis, presenting an important avenue for future research.

In conclusion, our study establishes LINC01980 as a significantly upregulated lncRNA in LSCC with potential diagnostic value. The proposed ceRNA network provides a foundation for future mechanistic studies to unravel the complex role of LINC01980 in LSCC pathogenesis. As research in this field progresses, LINC01980 may emerge as a promising target for novel diagnostic and therapeutic strategies in LSCC management.

Acknowledgments

We would like to express our gratitude to the AmirAlam Hospital Otorhinolaryngology Research Center for providing the patient samples that enabled this study. This work was supported by a research grant (Grant Number: 1401-3-366-63791) from the Faculty of Medicine, Tehran University of Medical Sciences (TUMS),

[DOI: 10.22088/IJMCM.BUMS.14.1.517]

Tehran, Iran. We sincerely appreciate this funding opportunity. Additionally, we would like to extend our appreciation to all the individuals who participated in our research.

References

1. Steuer CE, El-Deiry M, Parks JR, et al. An update on larynx cancer. CA Cancer J Clin 2017;67:31-50.

2. Bray F, Laversanne M, Sung H, et al. Global cancer statistics 2022: GLOBOCAN estimates of incidence and mortality worldwide for 36 cancers in 185 countries. CA Cancer J Clin 2024;74:229-63.

3. Bartonicek N, Maag JL, Dinger ME. Long noncoding RNAs in cancer: mechanisms of action and technological advancements. Mol Cancer 2016;15:43.

4. Bhan A, Soleimani M, Mandal SS. Long Noncoding RNA and Cancer: A New Paradigm. Cancer Res 2017;77:3965-81.

5. Huarte M. The emerging role of lncRNAs in cancer. Nat Med 2015;21:1253-61.

6. Liang X, Wu Z, Shen S, et al. LINC01980 facilitates esophageal squamous cell carcinoma progression via regulation of miR-190a-5p/MYO5A pathway. Arch Biochem Biophys 2020;686:108371.

7. Zhang S, Liang Y, Wu Y, et al. Upregulation of a novel lncRNA LINC01980 promotes tumor growth of esophageal squamous cell carcinoma. Biochem Biophys Res Commun 2019;513:73-80.

8. Sheng J, Luo Y, Lv E, et al. LINC01980 induced by TGF-beta promotes hepatocellular carcinoma metastasis via miR-376b-5p/E2F5 axis. Cell Signal 2023;112:110923.

9. Zang Y, Yi Q, Pan J, et al. LINC01980 stimulates the progression of hepatocellular carcinoma via downregulating caspase 9. J buon 2020;25:1395-403.

10. Zhao S, Li P, Zhou G. Long Noncoding RNAs in the Prediction of Survival of Patients with Digestive Cancers. Turk J Gastroenterol 2023;34:19-25.

11. Li M, Zhao LM, Li SL, et al. Differentially expressed lncRNAs and mRNAs identified by NGS analysis in colorectal cancer patients. Cancer Med 2018;7:4650-64.

12. Lin LT, Chang CY, Chang CH, et al. Involvement of let-7 microRNA for the therapeutic effects of Rhenium-188-embedded liposomal nanoparticles on orthotopic human head and neck cancer model. Oncotarget 2016;7:65782-96.

13. Mitra D, Das PM, Huynh FC, Jones FE. Jumonji/ARID1 B (JARID1B) protein promotes breast tumor cell cycle progression through epigenetic repression of microRNA let-7e. J Biol Chem 2011;286:40531-5.

14. Zhu W-Y, Luo B, An J-y, et al. Differential expression of miR-125a-5p and let-7e predicts the progression and prognosis of non-small cell lung cancer. Cancer Invest 2014;32:394-401.

15. Xiao M, Cai J, Cai L, et al. Let-7e sensitizes epithelial ovarian cancer to cisplatin through repressing DNA double strand break repair. J Ovarian Res 2017;10:1-13.

16. Shi W, Zhang Z, Yang B, et al. Overexpression of microRNA let-7 correlates with disease progression and poor prognosis in hepatocellular carcinoma. Med (Baltimore) 2017;96:e7764.

17. Chen W, Lin G, Yao Y, et al. MicroRNA hsa-let-7e-5p as a potential prognosis marker for rectal carcinoma with liver metastases. Oncol lett 2018;15:6913-24.

18.Ma J, Zhan Y, Xu Z, et al. ZEB1 induced miR-99b/let-7e/miR-125a cluster promotes invasion and metastasis in esophageal squamous cell carcinoma. Cancer Lett 2017;398:37-45.

19. Hilly O, Pillar N, Stern S, et al. Distinctive pattern of let-7 family microRNAs in aggressive carcinoma of the oral tongue in young patients. Oncol Lett 2016;12:1729-36.

20. Wang S, Jin S, Liu M-D, et al. Hsa-let-7e-5p inhibits the proliferation and metastasis of head and neck squamous cell carcinoma cells by targeting chemokine receptor 7. J Cancer 2019;10:1941.

[DOI: 10.22088/IJMCM.BUMS.14.1.517]

21. Huang Q, Yang J, Zheng J, et al. Characterization of selective exosomal microRNA expression profile derived from laryngeal squamous cell carcinoma detected by next generation sequencing. Oncol Rep 2018;40:2584-94.
22. Ventayol M, Viñas JL, Sola A, et al. miRNA let-7e targeting MMP9 is involved in adipose-derived stem cell differentiation toward epithelia. Cell Death Dis 2014;5:e1048.
23. Gkouveris I, Nikitakis NG, Aseervatham J, et al. Matrix metalloproteinases in head and neck cancer: current perspectives. Metalloproteinases Med 2017:47-61.
24. Virós D, Camacho M, Zarraonandia I, et al. Prognostic role of MMP-9 expression in head and neck carcinoma patients treated with radiotherapy or chemoradiotherapy. Oral Oncol 2013;49:322-5.
25. Lin M, Ashraf NS, Mahjabeen I. Deregulation of MMP-2 and MMP-9 in laryngeal cancer: A retrospective observational study. Med (Baltimore) 2024;103:e38362.
26. Gou X, Chen H, Jin F, et al. Expressions of CD147, MMP-2 and MMP-9 in Laryngeal Carcinoma and its Correlation with Poor Prognosis. Pathol Oncol Res 2014;20:475-81.
27. Rashid ZA, Bardaweel SK. Novel Matrix Metalloproteinase-9 (MMP-9) Inhibitors in Cancer Treatment. Int J Mol Sci 2023;24.
28. Tune BXJ, Sim MS, Poh CL, et al. Matrix Metalloproteinases in Chemoresistance: Regulatory Roles, Molecular Interactions, and Potential Inhibitors. J Oncol 2022;2022:3249766.

[DOI: 10.22088/IJMCM.BUMS.14.1.517]